

# Thermal and Three-body Abrasion Behaviors of Alkali-treated Eucalyptus Fiber Reinforced Polyvinyl Chloride Composites

Keping Zhang,\* Yongting Cui, and Wenbin Yan

Wood-plastic composites (WPCs) have been widely used as exterior construction materials. The effect of alkali-treated (with NaOH concentrations of 1%, 3%, 5%, and 7%) eucalyptus fiber on the three-body abrasion behaviors of eucalyptus/polyvinyl chloride (PVC) composites was investigated. The results showed that the eucalyptus fiber treated with NaOH had a higher crystallinity and improved hardness and impact strength. The wear loss and rate of alkali-treated eucalyptus/PVC composites was noticeably decreased compared to the natural eucalyptus fiber. The scanning electron microscopy (SEM) examination on the worn surfaces revealed that the main wear mechanism of the eucalyptus/PVC composites was a combination of microcutting and microindentations.

*Keywords:* Eucalyptus; Natural fiber composites; Alkali treatment; Three-body abrasion; Wear

*Contact information:* College of Mechanical and Electrical Engineering, Gansu Agricultural University, Lanzhou 730070, China; \* Corresponding author: zhangkp@gsau.edu.cn

## INTRODUCTION

Wood-plastic composites (WPCs) are green biomaterials that are manufactured by injection, extrusion, or moulding that use plant fibers as reinforcement and thermoplastic plastics as the matrix (Félix *et al.* 2013; Lin *et al.* 2017). In recent years, WPCs have been widely used as exterior construction materials, such as decking and fencing (Catto *et al.* 2016; Jiang *et al.* 2018b). However, the WPCs used in most of the above fields are inevitably subject to three-body abrasion, and therefore it is necessary to study the three-body abrasive wear behavior of WPCs to improve their wear resistance.

Recently, two-body wear behavior analyses of WPCs based on plant fibers, such as wheat straw (Jiang *et al.* 2017), rice straw (Jiang *et al.* 2017), corn straw (Jiang *et al.* 2017), sorghum straw (Jiang *et al.* 2017, 2018a), bamboo (Nirmal *et al.* 2012), kenaf (Chin and Yousif 2009), sugarcane (El-Tayeb 2008), cotton (Hashmi *et al.* 2007), and jute (Chand and Dwivedi 2006), have been performed. Eucalyptus, a type of high quality and high yield tree, has become one of the most important afforestation tree species in the global man-made forest, effectively solving the current shortage of timber. However, there have been few studies on the three-body abrasion behaviors of the eucalyptus-plastic composites.

One important method for enhancing the wear resistance of WPCs and the interfacial bonding of natural fibers with a polymer matrix is NaOH treatment, while other techniques have exhibited either no effect or deterioration of the fiber strength (Alawar *et al.* 2009; Phuong *et al.* 2010; Saha *et al.* 2010; Yousif *et al.* 2010; Jiang *et al.* 2018a). Sorghum straw (SS) fiber treated with 4.5% NaOH showed a low polarity and hydrophilicity with high crystallinity and improved mechanical properties, which endowed the SS/PVC composites with high interfacial bonding and wear resistance (Jiang *et al.* 2018a).

This study aims to explore the three-body abrasion behaviors of alkali-treated eucalyptus fiber-reinforced polyvinyl chloride composites. These results will supplement the three-body abrasion behaviors of WPCs in outdoor applications.

## EXPERIMENTAL

### Materials

Eucalyptus (*Eucalyptus robusta* Smith) was purchased from Guangxi Fenglin Wood Industry Co., Ltd., Guangxi, China. The density is  $0.611 \text{ g}\cdot\text{cm}^{-3}$ . The main chemical composition includes fibrin (42.31%), half-fibrin (16.65%), lignin (24.38%) and ash (4.38%). The SG-5 polyvinyl chloride (PVC) was purchased from Tianjin Tongxingguo Trading Co., Ltd., Tianjin, China. The 400A maleic anhydride graft coupling agent and 603 non-toxic Ca/Zn composite stabilizer were purchased from Guangzhou Yinghong Chemical Co., Ltd., Guangzhou, China. The H-108 PE (polyethylene) wax was purchased from Wujiang Meiqi Plastic Material Co., Ltd., Suzhou, China.

### *Eucalyptus fiber and WPC sample preparation*

The air-dried eucalyptus was initially crushed, subsequently ground, and finally filtered with a 100-mesh screen (149  $\mu\text{m}$  pore size). Selected eucalyptus fibers were soaked in 1%, 3%, 5%, and 7% NaOH concentrations at 100 °C for 1 h (solid-liquid ratio = 1:2). The treated fibers were separated from the liquid by filtration and washed with deionized water until the rinsed solution became neutral. The rinsed fibers were then dried at 90 °C for 16 h in a DHG-9055A electrical thermostatic drum-wind drying oven (Shanghai Yiheng Scientific Instrument Co., Ltd., Shanghai, China), then cooled to room temperature in the oven, obtaining a moisture content of less than 3%.

Based on the pre-experiment data, the alkali-treated eucalyptus fiber, PVC, coupling agent, stabilizer, and PE wax (mass ratio = 100:100:3:8:5, respectively) were mixed in a SYH-5 3D linkage mixer (Changzhou Feima Drying Equipment Co., Ltd., Changzhou, China). The compound was then placed into a SY-6216 intermeshing twin-screw extruder (Shiyan Precision Instruments Co., Ltd., Guangdong, China). During the extrusion, the temperature profiles from the hopper to die zone were controlled at 150, 155, 160, and 165 °C, and the rotational speed of the screw was 20 rpm. The extruded samples had a width and thickness of 25.5 mm and 6 mm, respectively, and the density of the samples is  $2.355 \text{ g}\cdot\text{cm}^{-3}$ . The lengths of the WPCs were verified and controlled by the extrusion period. The solidified samples were cut to a length of 57 mm with a hand saw for further testing.

### Methods

#### *Physicochemical properties of the eucalyptus fiber*

The crystal structures of the eucalyptus fibers were characterized using an XRD-6000 X-ray diffractometer (XRD; Shimadzu (China) International Trade, Co., Ltd., Tianjin) with a Cu radiation source, at an accelerating voltage of 50 KV and applied current of 60 mA. The specimens were scanned at a speed of  $0.33^\circ\cdot\text{min}^{-1}$ , with  $2\theta$  ranging from  $0^\circ$  to  $90^\circ$ . The crystallinity index (*CrI*) was calculated using Eq. 1 (Abdul *et al.* 2016; Jiang *et al.* 2018a),

$$CrI = [1 - (I_{am}/I_{002})] \times 100 \quad (1)$$

where  $I_{am}$  is the intensity of the amorphous phase ( $2\theta = 18^\circ$ ), and  $I_{002}$  is the intensity of the crystalline phase peak at  $2\theta = 22.5^\circ$ , which essentially consists of cellulose substances.

The chemical structures of the eucalyptus fibers were characterized using a NEXUS 670 Nicolet Fourier transform infrared (FTIR) spectrometer (Thermo Fisher Scientific (China) Co., Ltd., Shanghai). The measurements were performed over the range 400 to 4000  $\text{cm}^{-1}$ , with a resolution of 4  $\text{cm}^{-1}$ , and the results were an average of value of 16 scans.

#### *Physical and mechanical properties of the eucalyptus/PVC composites*

The hardness tests were performed in accordance with the Chinese standard GB/T 3398.1 (2008). Using a XHR-150 Plastics Rockwell hardness tester (Suzhou Nanguang Electronic Technology Co., Ltd., Suzhou, China) with an HRR (Rockwell hardness) ruler, the indenter diameter was determined as 12.7 mm. The loading and unloading times were both 15 s, and a load of 60 kg was applied for a period of 5 s.

The impact stress was evaluated using a digital impact tester (XJJ-5; Xiamen Forbs Testing Instrument Co., Ltd., Xiamen, China) at an impact energy of 2.75 J, according to GB/T 1043.1 (2008).

The results of the physical and mechanical properties are the average value of five independent measurements at room temperature ( $20 \pm 1^\circ\text{C}$ ).

#### *Three-body wear test of the eucalyptus/PVC composites*

The three-body wear tests were performed on a rubber rimmed wheel three-body sand abrasive wear tester (MLS-225; Zhangjiakou Taihua Machine Co., Ltd., Zhangjiakou, China) at room temperature ( $20 \pm 1^\circ\text{C}$ ). The sand abrasives were sourced from the Yellow River in Lanzhou, China. The sand was washed, air-dried, and filtered with a 36-mesh screen (0.5-mm pore size). The Shore hardness of the rimmed rubber was A-70 degree and the circumference of the wheel was 0.559 m. During the test, the specimen ( $6 \times 25.5 \times 57 \text{ mm}^3$ ) was pressed against the rimming rubber wheel by dead-weight loading, which was set to 225 N. The rotational speed of the rubber wheel was set to 300  $\text{r} \cdot \text{min}^{-1}$ , approximately 2.8  $\text{m} \cdot \text{s}^{-1}$  in linear velocity, and a wear time of 20 min. Prior to and following each test, the surfaces of the specimen were cleaned with absolute ethanol and air-dried. A minimum of three specimens were tested for each test with satisfactory repeatability.

The specific wear rate ( $W_s$ ) was calculated using Eq. 2 (Jeantrakull *et al.* 2012), by determining the weight loss and density of the test specimen. The weight loss of the test specimen was measured using an AUY 220 electronic analytical balance (Shimadzu (China) International Trade, Co., Ltd., Tianjin, China) with an accuracy of 0.1 mg. The density of the test specimen was measured using a TD-120 high precision touch screen plastic density tester (Taizhou Tiande Instrument Equipment Co., Ltd., Taizhou, China),

$$W_s = \frac{\Delta M}{LF\rho} \quad (2)$$

where  $\Delta M$  is the weight loss (mg),  $L$  is the sliding distance (m),  $F$  is the applied load (N), and  $\rho$  is the specimen density ( $\text{g} \cdot \text{cm}^{-3}$ ).

#### *Thermogravimetric and morphological analysis of the eucalyptus/PVC composites*

The thermogravimetric (TG) analyses of the eucalyptus/PVC composites were performed by a ZH-1000 comprehensive thermal analyzer (Shanghai Innuo Precision Instrument Co., Ltd., Shanghai, China). The gas flow rates of the shielding gas and sweep

gas were  $20 \text{ mL}\cdot\text{min}^{-1}$  and  $60 \text{ mL}\cdot\text{min}^{-1}$ , respectively. The tests were conducted over the temperature range of 30 to  $800 \text{ }^\circ\text{C}$  at a heating rate of  $20 \text{ }^\circ\text{C}\cdot\text{min}^{-1}$ . The weights of all specimens were maintained at 5 to 10 mg.

Morphological analysis of the eucalyptus/PVC composites' worn surfaces were performed by a JSM-5600LV scanning electron microscopy (SEM) (JEOL Ltd., Tokyo, Japan). Prior to the SEM analysis, the worn surfaces of the specimens were coated with gold by an E-1010 ion sputter coater (JEOL Ltd., Tokyo, Japan).

## RESULTS AND DISCUSSION

### Physicochemical Properties of the Eucalyptus Fiber

The crystallinity of cellulose affects the physical, mechanical, and chemical properties of plant fiber, and the plant fiber with higher crystallinity has a better hardness, Young's modulus, and dimensional stability (Ju *et al.* 2015; Caliarì *et al.* 2017). The XRD spectra of the eucalyptus fibers are shown in Fig. 1. The crystallinity index of the untreated, 1%, 3%, 5%, and 7% alkali-treated eucalyptus fibers were 42.9, 43.8, 45.5, 49.2, and 48.2%, respectively. The maximum crystallinity was observed in the fiber with the 5% NaOH treatment. A small difference between the fiber with 1% NaOH treatment and the untreated one was observed. In other words, lower concentrations of NaOH did not change the structure of the fiber dramatically.

According to Fig. 1, the diffraction peaks around  $2\theta$  of  $15^\circ$  and  $22^\circ$  were observed in all treated and untreated eucalyptus fibers, which corresponded to the typical pattern of the cellulose-I structure.

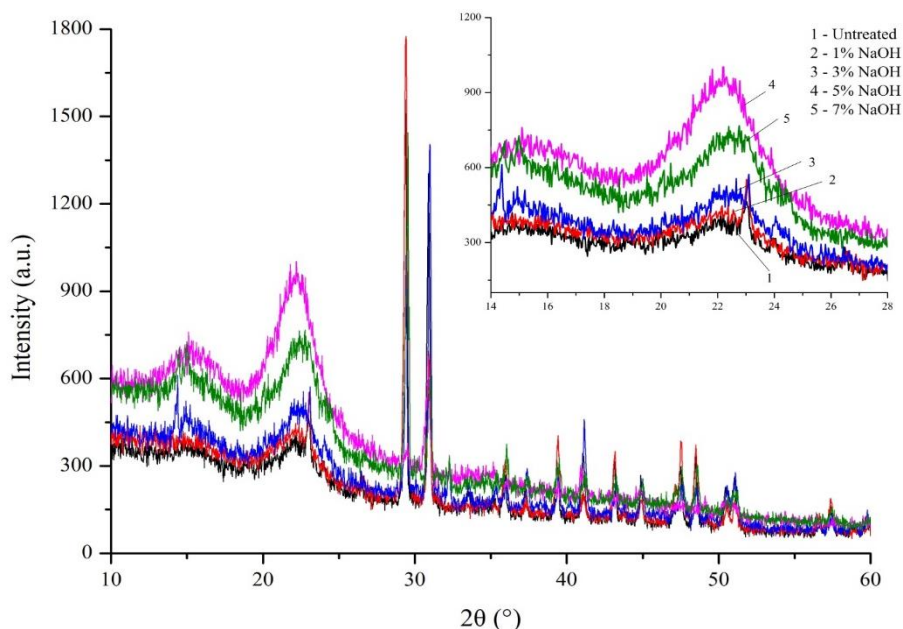


**Fig. 1.** XRD spectra of eucalyptus fibers

During alkali-treatment, non-cellulosic material, such as hemicelluloses, lignin, pectin, and soluble polysaccharides, were removed. Therefore, the crystallinity index of the eucalyptus fibers increased as the concentration of NaOH increased from 1% to 5%.

However, with 7% NaOH treatment, the main structural components of the eucalyptus fibers were destroyed, such as hydrogen bonds, and led to the dissolution of some plants' crystalline regions, resulting in a loss of conformation and crystallinity. It has been shown that the crystallinity index of sorghum straw fiber with 6.5% NaOH treatment was lower than that of the 4.5% NaOH treatment samples (Jiang *et al.* 2018a). The results observed in this study were also in accordance with other research (Oudiani *et al.* 2011).

The FTIR spectra of the eucalyptus fibers are shown in Fig. 2. The absorption peak of 3500 to 3300  $\text{cm}^{-1}$  showed the stretching vibration of -OH in the cellulose, hemicellulose, polysaccharide, and monosaccharide. The absorption peak of 2935 to 2900  $\text{cm}^{-1}$  showed the C-H asymmetric stretching vibration of -CH<sub>3</sub>- and -CH<sub>2</sub>- in cellulose. The peak of 1735 to 1700  $\text{cm}^{-1}$  indicated that the C=O stretching vibration of esters and ketones was related to lignin or hemicellulose. The peak of 1515 to 1505  $\text{cm}^{-1}$  was the stretching vibration of the benzene-ring skeleton. The peak of 1250 to 1230  $\text{cm}^{-1}$  was the stretching vibration of C-O in lignin and the stretching vibration of Si-C in the organosilicon compound, and the peak of 1100 to 970  $\text{cm}^{-1}$  showed the stretching vibrations of -C-O in the polysaccharide (Jiang *et al.* 2017). All peaks were typical peaks for the absorption of plant fibers. The FTIR spectra proved that all samples of eucalyptus fibers had similar chemical functional groups, which suggested that the main functional groups did not change under the alkali treatment. However, the transmittance of all the typical peaks increased with increasing NaOH concentration, indicating the decrease of polarity and hydrophilicity in eucalyptus fibers. The results were consistent with the references (Oushabi *et al.* 2017; Jiang *et al.* 2018a). In addition, the peaks at 1740 and 1250  $\text{cm}^{-1}$  completely disappeared during the 3% to 7% NaOH treatment, proving that the alkali treatment removed the functional groups related to hemicellulose, lignin, or pectin in eucalyptus fibers (Krishnaiah *et al.* 2017). However, the spectra of fiber with 1% NaOH treatment was similar to that of the untreated fiber, which meant that NaOH with a lower concentration did not change the structure of the fiber (XRD showed the same result).

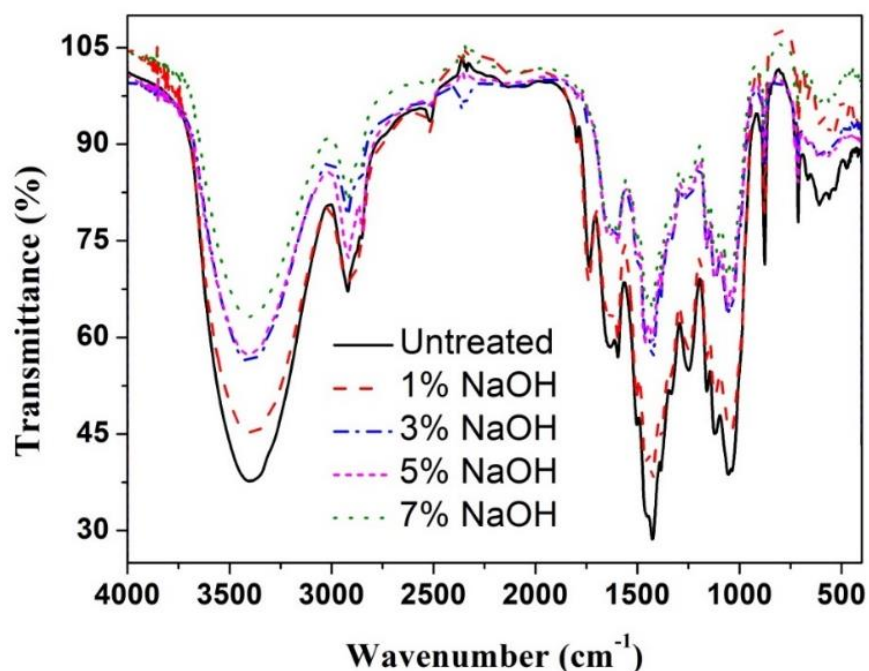
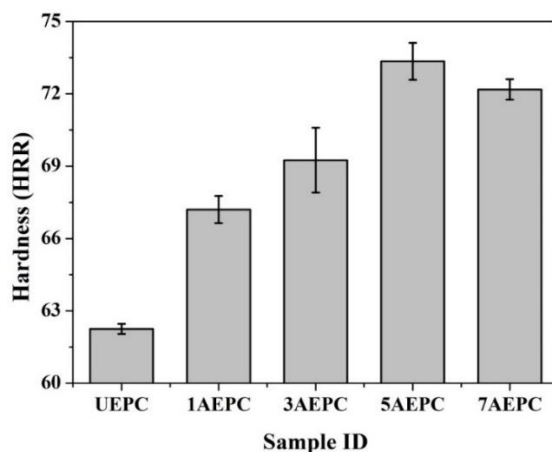


Fig. 2. FTIR spectra of the eucalyptus fibers

### Hardness and impact strength of the Eucalyptus/PVC Composites

Hardness of a material is one of the important physical properties that may affect the three-body abrasion. Figure 3 shows the hardness of eucalyptus/PVC composites with different alkali treatment concentrations. Compared to the treated fibers, the natural eucalyptus/PVC composites had the lowest hardness ( $62.26 \pm 0.21$ ), and the hardness of composites increased with the increasing concentration of alkali from 1% to 5%. The highest hardness was found in the fiber with 5% NaOH treatment ( $73.35 \pm 0.77$ ). Compared to the raw fiber, the hardness of 5% NaOH-treated eucalyptus/PVC composites had a 17.8% increase. Under 7% NaOH treatment, the hardness of eucalyptus/PVC composites decreased, but was still higher than what was observed during the 3% NaOH treatment. Due to the removal of hemicelluloses, lignin, pectin, monosaccharide, and soluble polysaccharide by alkali treatment, the components of the fiber changed. The main component of treated fiber was cellulose, which had a higher hardness. Therefore, the hardness of fiber enhanced with alkali treatment. It has been proven that the massive alkali could not only remove the non-cellulose components, but also dissolve the crystalline regions, resulting in the reduction of the fiber's hardness (Jiang *et al.* 2018a).



**Fig. 3.** Hardness of the eucalyptus /PVC composites

The impact strength of material is one of the important mechanical properties that may affect the three-body abrasion. The impact strengths of the untreated and alkali-treated eucalyptus fibers are shown in Fig. 4. Compared with the natural eucalyptus fibers, the impact strength of the fibers was enhanced by the application of a mild alkali treatment, due to the removal of hemicelluloses, lignin, and other impurities. A small amount of impurities led to a more regular structure of fibers. Therefore, the impact strength of eucalyptus fibers was improved by alkali, which was in accordance with the references (Phuong *et al.* 2010; Saha *et al.* 2010; Jiang *et al.* 2018a). The eucalyptus fibers with 5% NaOH treatment had the highest impact strength among all of the samples. The 39.8% increase in impact strength was observed in the fiber with a 5% concentration alkali treatment, compared to the raw fiber. However, the 7% NaOH-treated eucalyptus fiber had a lower impact strength than that of the 5% NaOH-treated fiber. Excessive alkali could destroy the hydrogen bonds among the cellulose molecules, which contributed to its structural stability. The impact strength of the fibers decreased with the decrease in the cellulose's structural stability. The results from XRD and FTIR of eucalyptus fibers were highly consistent with the results of hardness and impact strength.



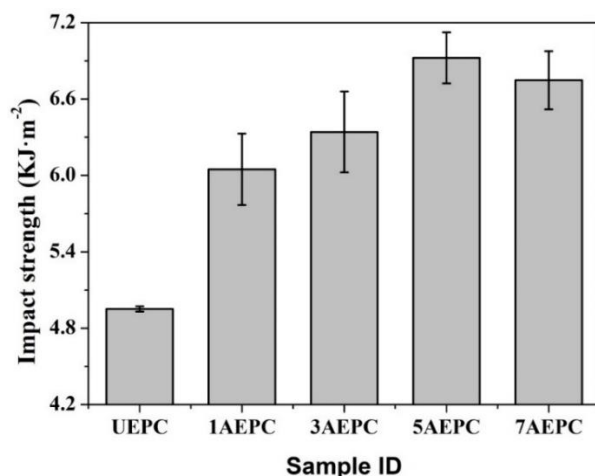


Fig. 4. Impact strength of the eucalyptus/PVC composites

### Fracture Surfaces Analysis of the Eucalyptus/PVC Composites

SEM micrographs of the impact fracture surfaces of the untreated (UEPC) and alkali-treated eucalyptus/PVC composites with 5% NaOH (5AEPC) are shown in Fig. 5. Compared with the untreated eucalyptus/PVC composites (Fig. 5a), fewer fibers were exposed to the outside, and more fibers were embedded in the matrix (Fig. 5b). Meanwhile, the holes and gaps between the fibers and the matrix were lesser, indicating that the dispersion and compatibility between the fiber and matrix were better with the alkali treatment.

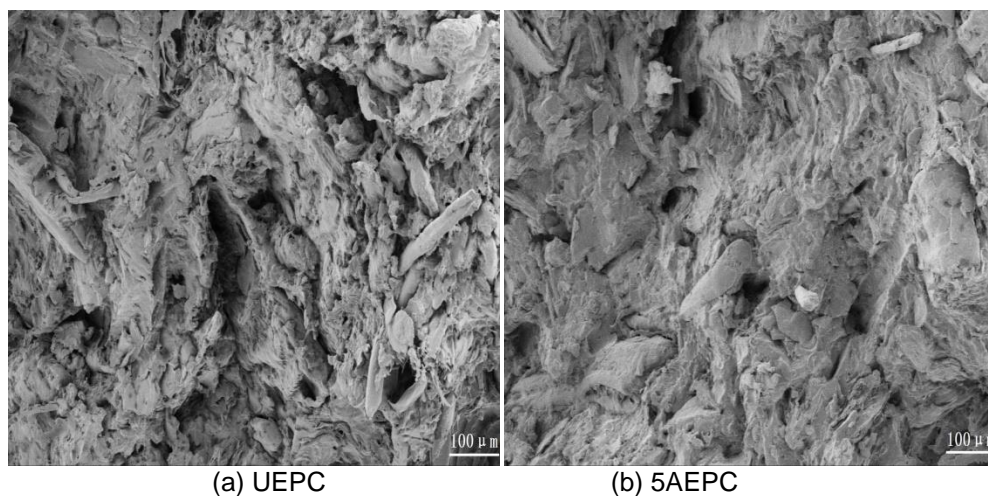


Fig. 5. SEM micrographs of the impact fracture surfaces of the UEPC and 5AEPC

### TGA of the Eucalyptus/PVC Composites

The high thermo-mechanical loading between the interacting surfaces of the counterpart and the test sample caused dry sliding with high velocity, high load, and long distance. As a result, the temperature increased. The high temperature could soften the polymer matrix leading to the poor interfacial bonding strength and subsequent high material removal (Jiang *et al.* 2018a). Since the temperature always increases on the

interacting surfaces of three-body abrasion, the thermal stability is one of the important properties of the polymers that could affect the three-body abrasion.

The TG curves and pyrolysis characteristic data of the eucalyptus/PVC composites are shown in Fig. 6 and Table 1, respectively. It can be seen that there were two significant mass loss stages during the heating process for all composites. The first stage (approximately 260 to 340 °C) with a high mass loss of 50.2% to 54.6% showed the thermal degradation of cellulose, hemicellulose, and lignin. The lower mass loss of 14.7% to 18.4% in the second stage (approximately 450 to 500 °C) was due to the thermal degradation of the PVC carbon chain, which produced flammable volatiles. The mass loss in both stages decreased as the content of NaOH increased and the composite with 7% NaOH treatment eucalyptus fibers had the lowest weight loss among all the samples. Because the alkali-treated fibers were able to distribute into the PVC more homogeneously than the untreated fibers, which absorb energy during heating, less energy was transmitted to the PVC and the TG values of the samples increased with an increase in NaOH concentration (Monteiro *et al.* 2012; Jiang *et al.* 2018a).

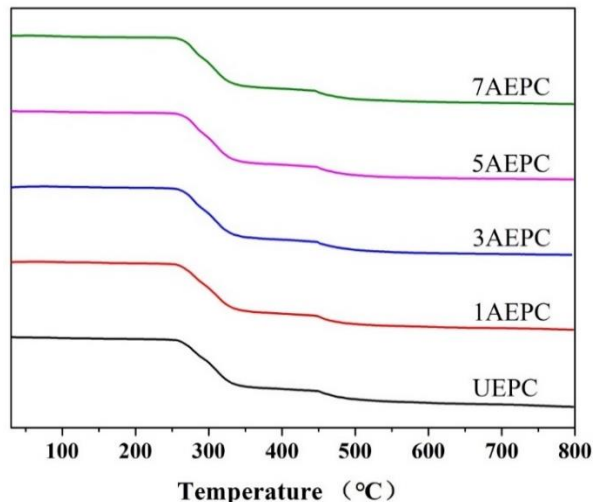


Fig. 6. TG curves of the eucalyptus/PVC composites

Table 1. Pyrolysis Characteristic Data of the Eucalyptus/PVC Composites

Sample ID	Pyrolysis Process					
	First Stage			Second Stage		
	Temperature (°C)		Mass Loss (%)	Temperature (°C)		Mass Loss (%)
	Onset	Termination		Onset	Termination	
UEPC	254.6	326.1	54.6	446.9	472.8	18.4
1AEPC	259.7	328.4	54.3	448.9	476.6	16.8
3AEPC	263.6	328.9	53.1	450.3	478.6	15.8
5AEPC	264.5	330.1	52.1	450.4	481.3	15.4
7AEPC	266.9	331.5	50.2	451.2	484.4	14.7

### Wear Properties of the Eucalyptus/PVC Composites

The three-body abrasive wear mass loss and wear rates of eucalyptus/PVC composites are shown in Table 2. Compared with UEPC, the wear resistance of the composites clearly improved with the alkali-treatment. The wear resistance increased in the following order: UAEPCC > 1AEPC > 3AEPC > 7AEPC > 5AEPC. The  $W_s$  value of



5AEPC was the lowest compared to the other samples, which could have been attributed to the high crystallinity and strength of the eucalyptus fibers and the stronger interfacial bonding with the PVC matrix of treated fiber at a 5% NaOH concentration. This led to stronger load-bearing fiber and required more energy for de-bonding of the fiber/matrix interface.

**Table 2.** Three-body Abrasion Wear Results

Sample ID	Mass Loss (mg)	$Ws$ ( $\text{mm}^3/\text{Nm}$ ) $\times 10^{-5}$
UEPC	$178 \pm 18$	$10.0 \pm 0.3$
1AEPC	$143.1 \pm 25$	$8.1 \pm 0.4$
3AEPC	$119.0 \pm 21$	$6.7 \pm 0.4$
5AEPC	$92.1 \pm 15$	$5.2 \pm 0.3$
7AEPC	$115.1 \pm 30$	$6.5 \pm 0.6$

### Wear Mechanisms of the Eucalyptus/PVC Composites

The SEM micrographs of the three-body abrasive typical worn surfaces of the UEPC and 5AEPC are shown in Fig. 7. The obvious abrasive wear features, such as furrows and pits, could be seen clearly on the worn surfaces. The massive furrows on the worn surfaces should be generated from the linear travel of sand abrasives and a few pulled-out fibers that were driven by the rotating wheel. In particular, the sand abrasives between the interface were pressed onto the wear surface by normal force and cut (or pushed) the wear surface as the cutter forward in an angle under the driving force of tangential force. Thus, furrows, pits, and fiber fragments were distributed along the moving path of the abrasives, the main wear mechanism was a combination of microcutting and microindentations (Ren *et al.* 2014; Penagos *et al.* 2015). It should be noted that the furrows and pits in Fig. 7(b) were shallower and smoother than those in Fig. 7(a), which meant an increase in wear resistance was observed from the 5AEPC surface to the UEPC surface. This was mainly because of the NaOH treatment on the crystallization, fiber strength, and pull-out resistance of eucalyptus fibers.

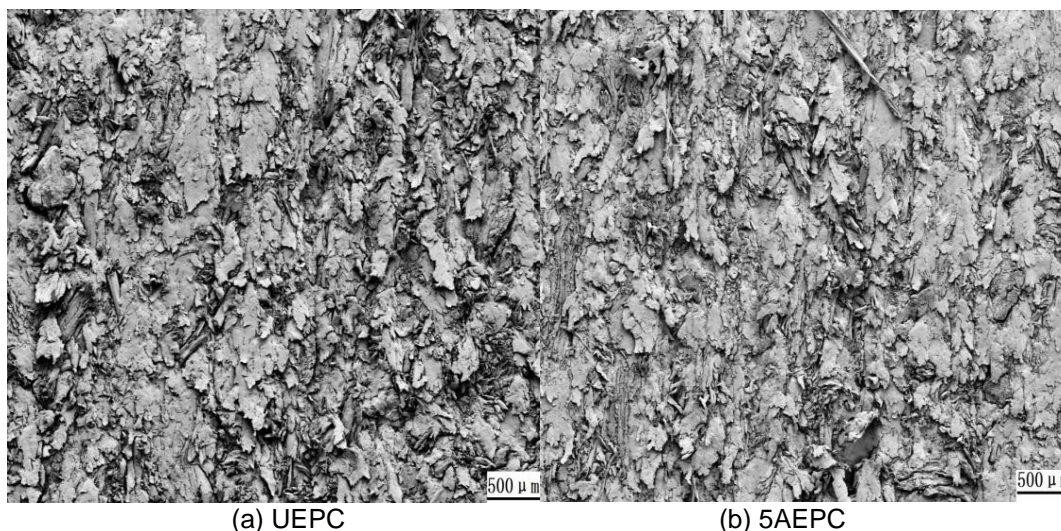


**Fig. 7.** SEM micrographs of the worn surfaces of the UEPC and 5AEPC

## CONCLUSIONS

1. The three-body abrasive wear resistance of alkali-treated eucalyptus fiber/PVC composites was improved compared to the untreated eucalyptus fiber.
2. The NaOH treatment yielded a high crystallinity for eucalyptus fibers and improved the hardness and impact strength for eucalyptus/PVC composites. The 5% alkali-treated eucalyptus fiber endowed the highest interfacial bonding and wear resistance to the eucalyptus/PVC composites, compared with the other samples.

## ACKNOWLEDGEMENTS

This work was supported by the Discipline Construction Fund Project of Gansu Agricultural University, Grant No. GAU-XKJS-2018-191 and the Fund for Young Supervisor of Gansu Agricultural University, Grant No. GAU-QNDS-201711.

## REFERENCES CITED

- Abdul, P. M., Jahim, J. M., Harun, S., Markom, M., Lutpi, N. A., Hassan, O., Balan, V., Dale, B. E., and Mohd Nor, M. T. (2016). "Effects of changes in chemical and structural characteristic of ammonia fibre expansion (AFEX) pretreated oil palm empty fruit bunch fibre on enzymatic saccharification and fermentability for biohydrogen," *Bioresource Technology* 211, 200-208. DOI: 10.1016/j.biortech.2016.02.135
- Alawar, A., Hamed, A. M., and Al-Kaabi, K. (2009). "Characterization of treated date palm tree fiber as composite reinforcement," *Composites Part B: Engineering* 40(7), 601-606. DOI: 10.1016/j.compositesb.2009.04.018
- Caliari, I. P., Barbosa, M. H. P., Ferreira, S. O., and Teófilo, R. F. (2017). "Estimation of cellulose crystallinity of sugarcane biomass using near infrared spectroscopy and multivariate analysis methods," *Carbohydrate Polymers* 158, 20-28. DOI 10.1016/j.carbpol.2016.12.005
- Catto, A. L., Montagna, L. S., Almeida, S. H., Silveira, R. M. B., and Santana, R. M. C. (2016). "Wood plastic composites weathering: Effects of compatibilization on biodegradation in soil and fungal decay," *International Biodeterioration & Biodegradation* 109, 11-22. DOI:10.1016/j.ibiod.2015.12.026
- Chand, N., and Dwivedi, U. K. (2006). "Effect of coupling agent on abrasive wear behaviour of chopped jute fibre-reinforced polypropylene composites," *Wear* 261(10), 1057-1063. DOI: 10.1016/j.wear.2006.01.039
- Chin, C. W., and Yousif, B. F. (2009). "Potential of kenaf fibres as reinforcement for tribological applications," *Wear* 267(9-10), 1550-1557. DOI: 10.1016/j.wear.2009.06.002
- El-Tayeb, N. S. M. (2008). "A study on the potential of sugarcane fibers/polyester composite for tribological applications," *Wear* 265(1-2), 223-235. DOI: 10.1016/j.wear.2007.10.006
- Félix, J. S., Domeño, C., and Nerín, C. (2013). "Characterization of wood plastic composites made from landfill-derived plastic and sawdust: Volatile compounds and

- olfactometric analysis,” *Waste Management* 33(3), 645-655. DOI: 10.1016/j.wasman.2012.11.005
- Hashmi, S. A. R., Dwivedi, U. K., and Chand, N. (2007). “Graphite modified cotton fibre reinforced polyester composites under sliding wear conditions,” *Wear* 262(11-12), 1426-1432. DOI: 10.1016/j.wear.2007.01.014
- Jeamtrakull, S., Kositchaiyong, A., Markpin, T., Rosarpitak, V., and Sombatsompop, N. (2012). “Effects of wood constituents and content, and glass fiber reinforcement on wear behavior of wood/PVC composites,” *Composites Part B: Engineering* 43(7), 2721-2729. DOI: 10.1016/j.compositesb.2012.04.031
- Jiang, L., He, C., Fu, J., and Chen, D. (2017). “Wear behavior of straw fiber-reinforced polyvinyl chloride composites under simulated acid rain conditions,” *Polymer Testing* 62, 373-381. DOI: 10.1016/j.polymertesting.2017.07.028
- Jiang, L., He, C., Fu, J., and Li, X. (2018a). “Wear behavior of alkali-treated sorghum straw fiber reinforced polyvinyl chloride composites in corrosive water conditions,” *BioResources* 13(2), 3362-3376. DOI: 10.15376/biores.13.2.3362-3376
- Jiang, L., He, C., Fu, J., and Wang, L. (2018b). “Serviceability analysis of wood-plastic composites impregnated with paraffin-based pickering emulsions in simulated sea water-acid rain conditions,” *Polymer Testing* 70, 73-80. DOI: 10.1016/j.polymertesting.2018.06.031
- Ju, X., Bowden, M., Brown, E. E., and Zhang, X. (2015). “An improved X-ray diffraction method for cellulose crystallinity measurement,” *Carbohydrate Polymers* 123, 476-481. DOI: 10.1016/j.carbpol.2014.12.071
- Krishnaiah, P., Ratnam, C. T., and Manickam, S. (2017). “Enhancements in crystallinity, thermal stability, tensile modulus and strength of sisal fibres and their PP composites induced by the synergistic effects of alkali and high intensity ultrasound (HIU) treatments,” *Ultrasonics Sonochemistry* 34, 729-742. DOI: 10.1016/j.ultsonch.2016.07.008
- Lin, X., Zhang, Z., Tan, S., Wang, F., Song, Y., and Wang, Q. (2017). “In line wood plastic composite pyrolyses and HZSM-5 conversion of the pyrolysis vapors,” *Energy Conversion and Management* 141, 206-215. DOI: 10.1016/j.enconman.2016.07.071
- Nirmal, U., Hashim, J., and Low, K. O. (2012). “Adhesive wear and frictional performance of bamboo fibres reinforced epoxy composite,” *Tribology International* 47, 122-133. DOI: 10.1016/j.triboint.2011.10.012
- Oudiani, A. E., Chaabouni, Y., Msahli, S., and Sakli, F. (2011). “Crystal transition from cellulose I to cellulose II in NaOH treated *Agave americana* L. fibre,” *Carbohydrate Polymers* 86(3), 1221-1229. DOI: 10.1016/j.carbpol.2011.06.037
- Oushabi, A., Sair, S., Hassani, F. O., Abboud, Y., Tanane, O., and Bouari, A. E. (2017). “The effect of alkali treatment on mechanical, morphological and thermal properties of date palm fibers (DPFs): Study of the interface of DPF-Polyurethane composite,” *South African Journal of Chemical Engineering* 23(01), 116-123. DOI: 10.1016/j.sajce.2017.04.005
- Penagos, J. J., Ono, F., Albertin, E., and Sinatora, A. (2015). “Structure refinement effect on two and three-body abrasion resistance of high chromium cast irons,” *Wear* 340-341, 19-24. DOI: 10.1016/j.wear.2015.03.020
- Phuong, N. T., Sollogoub, C., and Guinault, A. (2010). “Relationship between fiber chemical treatment and properties of recycled pp/bamboo fiber composites,” *Journal of Reinforced Plastics and Composites* 29(21), 3244-3256. DOI: 10.1177/0731684410370905

- Ren, X., Peng, Z., Hu, Y., Rong, H., Wang, C., Fu, Z., Qi, L., and Miao, H. (2014). “Three-body abrasion behavior of ultrafine WC-Co hard metal RX8UF with carborundum, corundum and silica sands in water-based slurries,” *Tribology International* 80, 179-190. DOI: 10.1016/j.triboint.2014.07.008
- Saha, P., Manna, S., Chowdhury, S. R., Sen, R., Roy, D., and Adhikari, B. (2010). “Enhancement of tensile strength of lignocellulosic jute fibers by alkali-steam treatment,” *Bioresource Technology* 101(9), 3182-3187. DOI: 10.1016/j.biortech.2009.12.010
- Yousif, B. F., Leong, O. B., Ong, L. K., and Jye, W. K. (2010). “The effect of treatment on tribo-performance of CFRP composites,” *Recent Patents on Materials Science* 2(1), 67-74. DOI: 10.2174/1874465610902010067

Article submitted: August 30, 2018; Peer review completed: December 15, 2018; Revised version received: December 17, 2018; Accepted: December 19, 2018; Published: December 20, 2018.

DOI: 10.15376/biores.14.1.1229-1240